ELSEVIER

Ceramics International 32 (2006) 163–172

CERAMICS INTERNATIONAL

www.elsevier.com/locate/ceramint

Hydration of coked MgO–C–Al refractories

S.K. Nandy [a,*], N.K. Ghosh [b], D. Ghosh [c], G.C. Das [c]

[a] *Research and Development Center for Iron and Steel (RDCIS) Kolkata Office, Steel Authority of India Limited (SAIL), 97 Park Street (2nd Floor), Kolkata 700016, West Bengal, India*

[b] *RTG, Research and Development Center for Iron and Steel (RDCIS), Steel Authority of India Limited (SAIL), P.O. Doranda, Ranchi 834002, India*

[c] *Department of Metallurgical and Material Engineering, Jadavpur University, Kolkata 700032, West Bengal, India*

Received 6 September 2004; received in revised form 26 October 2004; accepted 27 January 2005
Available online 25 April 2005

Abstract

Magnesia–carbon bricks collected from steel plants kept in open atmosphere were found to crack and disintegrate on prolonged exposure. To understand the mechanism of this behaviour, MgO–C–Al and Al–C samples were prepared, coked, and kept in open atmosphere. The samples crumbled to dust after few days. XRD showed the reduction of phases such as Al_4C_3, Al_4O_4C, Al_2O_3, and Al caused the disintegration with formation of amorphous phases. SEM showed the presence of hexagonal stack-like structures which converted to dust-like phases which EPMA identified as combination of aluminium and oxygen without the presence of carbon. Thermodynamic stability analysis for Al–O–C–H quaternary and Al–O–H ternary phase diagrams was done to explain the mechanism of hydration and consequent disintegration of coked MgO–C–Al bricks as well as Al–C samples on exposure to moist atmosphere at ambient temperature. On hydration, phases present in the coked samples convert to $Al(OH)_3$ which causes the disintegration.
© 2005 Elsevier Ltd and Techna Group S.r.l. All rights reserved.

Keywords: Magnesia–carbon–aluminium; Coking; Disintegration; Hydration; Thermodynamics

1. Introduction

Magnesia–carbon (MgO–C) refractories are considered to be the most cost-effective lining material for steel making furnaces. More specifically, MgO–C bricks are used extensively for the lining of basic oxygen furnaces (BOF) and in the slag zone of steel ladles for their good oxidation and slag resistance properties. Steel ladles are now being lined completely with MgO–C bricks. The role of carbon in magnesia–carbon refractories is attributed by many researchers [1–3] to their disinclination to be wetted by slags at high temperatures within the reacting vessel. Due to this property slag penetration is confined to a thin surface layer on the refractory. It is well known, additionally, that aluminium is added to MgO–C bricks to suppress carbon oxidation. In air, aluminium reacts the local environment to form Al_4C_3, AlN, Al_2O_3 and $MgAl_2O_4$ during the thermal treatment carried out at varying temperatures [4,5]. It is reported [6] that MgO–C–Al bricks have higher hot strength than MgO–C bricks, presumably due to the reinforcement caused by the aluminium carbide and other phases. Besides aluminium other metals such as silicon, alloys of aluminium and silicon and magnesium–aluminium alloys have been used with the MgO–C bricks [4,7] but Al is preferred and widely used in view of the excellent high temperature strength of the resulting MgO–C–Al bricks and its relatively low cost. However, MgO–C–Al brick suffers from some shortcomings.

For example, under damp conditions or in the presence of moisture, the Al_4C_3 reacts with the water vapour and expands enormously, making the brick crack and reducing its service life [8]. Further reports [9] reveal that refractory linings containing Al_4C_3 when kept at low or ambient temperatures, react with moisture to form $Al(OH)_3$ and CH_4 (methane), causing the disintegration of the bricks. However, a detailed study or a discussion about the mechanism of disintegration of the brick could not be found in the literature.

* Corresponding author. Tel.: +91 33 2227 1709; fax: +91 33 2227 1723.
E-mail address: sandipnandy@yahoo.co.in (S.K. Nandy).

0272-8842/$30.00 © 2005 Elsevier Ltd and Techna Group S.r.l. All rights reserved.
doi:10.1016/j.ceramint.2005.01.013

In BOF and steel ladles, some zones of the BOF and steel ladles are lined with MgO–C–Al bricks. However, there are occasions especially in steel ladles when they are cooled to ambient temperature for intermittent repairs, which may take several days. In rainy seasons, humidity is high and this may cause serious damage or deterioration of the costly linings presumably due to hydration of MgO–C–Al bricks. Such undesirable occurrences in extreme cases, may affect the production of a plant.

In Indian conditions of high humidity and ambient temperature, it is, therefore, necessary to study the hydration behaviour of MgO–C–Al refractories. In the present work, MgO–C–Al and Al–C samples were coked at 1050 °C and their disintegration behaviour was studied under different conditions at ambient temperature and the reaction products were analysed by XRD, IR, SEM and EPMA. These results and thermodynamic calculations were used to understand and explain the mechanism of hydration.

2. Experimental

2.1. Preparation of MgO–C–Al refractory samples

Refractory samples of MgO–C–Al were made by mixing high purity seawater magnesia (98.5% MgO) with graphite powders (95% fixed carbon) of 0.075–0.6 mm size and aluminum powders (99.9% purity chemical grade and 100% passing through 0.1 mm), bound by a resol type phenol formaldehyde liquid resin). Six coarse fractions of MgO grains of sizes 2.8–3.5, 2.0–2.8, 1.4–2.0, 1.0–1.4, 0.6–1.0, 0.25–0.6 mm and two fines fraction of 0.075–0.25 mm and −0.075 mm were taken for grain size distribution. Three batch compositions were prepared with/without aluminium powders as indicated in Table 1. Cylindrical samples of 25 mm diameter and 25 mm height were prepared at a specific pressure of 140 MPa and cured at 120 °C for 24 h. The green bulk densities of the cured samples varied from 2.85 to 2.88 g/cm^3.

2.2. Preparation of Al–C samples

To understand the mechanism of disintegration, experiments were carried out with samples containing Al and C only. Al–C samples of 25 mm diameter and 12–13 mm height were prepared by mixing the stoichiometric amounts of Al (108.5 g) and graphite (38.3 g) with phenol formaldehyde liquid resin and pressing at 80 MPa.

Table 1
Batch composition of MgO–C

Ingredient	*A* (%)	*B* (%)	*C* (%)
Magnesia	90	90	90
Graphite	10	10	10
Resin	4.5	4.5	4.5
Al powder	–	2	3

2.3. Coking of samples

MgO–C–Al and Al–C samples were then placed inside one stainless steel coking box and filled with petroleum coke. The box with the samples were then placed inside an electrically heated muffle furnace and the temperature was raised @5 °C/min to 1050 °C and hold for 3 h before furnace cooling to room temperature.

2.4. Weight changes in ambient temperature

Both the above two types of coked samples were kept in open conditions at ambient temperature (25–30 °C) and relative humidity (68–82%). Physical changes and weight of samples were noted at regular intervals for up to 60 days.

2.5. Observation under continuous flow of oxygen

This set of experiments was carried out with Al–C samples coked at 1050 °C in which moisture-free oxygen, obtained by passing oxygen from an oxygen cylinder (99% pure) through a series of $CaCl_2$ columns, flowed over the Al–C samples kept in an initially evacuated tube (to remove the moisture initially present in the system). The experiments were carried out at room temperature (varying from 25 to 30 °C) for 60 days. The samples were taken out and their weights were measured at regular intervals and the system was re-evacuated before the resumption of the experiment after each interruption for weight measurement.

2.6. X-ray diffraction

X-ray diffraction (XRD) was carried out on powder (<76 μm) samples before and after hydration using the Cu Kα monochromatic radiation with a Ni filter in a powder X-ray diffractometer (Bruker Axs, Germany) operated at 40 kV. The phase analysis was conducted with the EVA software provided with the equipment and the Siraquent (SQ) provided within the software conducted semi-quantitative analysis.

2.7. Infrared (IR) spectra study of Al–C samples

Al–C samples after coking at 1050 °C for 3 h were ground to <76 μm. The hydrated Al–C samples crumbled automatically to produce fines of size less than 76 μm. The IR spectra of these powder samples before and after hydration were taken over the range 500–5000 cm^{-1}.

2.8. Scanning electron microscope

A small part of the powdered samples previously used for IR characterization was placed on a brass holder and examined using a scanning electron microscope (Jeol-JSM-840A). Elements present in the test specimens were

identified by EDS (energy dispersive spectroscopy) attached to the SEM.

2.9. Electron probe micro analyser (EPMA)

The preceding specimens used for SEM studies were also observed under EPMA (Jeol super probe). Specimens were mapped for aluminum, carbon and oxygen.

3. Results and discussion

3.1. Disintegration of coked MgO–C containing Al

A used MgO–C brick containing Al was collected from the slag zone of a 150 T steel ladle during slag zone repair after 40 heats and kept in open conditions. Fine cracks appeared after 15 days and the brick gradually disintegrated on prolonged exposure. Fig. 1 shows the cracked brick after 20 days exposure. This phenomenon is of great concern as MgO–C bricks are sometimes kept for long periods after partial use in BOF and ladles. Water leakage from the BOF hood may also occur and damage these bricks. Chemical analysis of the brick after ignition revealed of about 5 wt.% Al_2O_3. As the complete history of the brick was unknown, it was decided to prepare MgO–C samples in the laboratory with various percentages of aluminium and study their disintegration behaviour.

Fig. 2 plots percent weight gain of these MgO–C samples as a function of time of exposure. It was observed that the higher the Al content in MgO–C samples, the higher is the percent weight gain for the same length of exposure. Fig. 3(a), (b), and (c), respectively, present the progressive superficial changes in MgO–C having 3% Al content samples after 1, 20, and 30 days of exposure. Samples having 3% Al crumbled in 30 days and developed visible cracks in 20 days, with little cracking after 1 day. By comparison, samples with 2% Al developed only fine hair

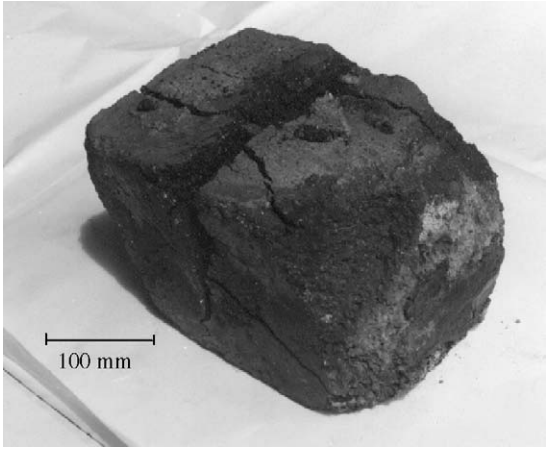

Fig. 1. Photograph of a typical disintegrated MgO–C brick collected from one integrated steel plant, after 20 days of exposure in open atmosphere.

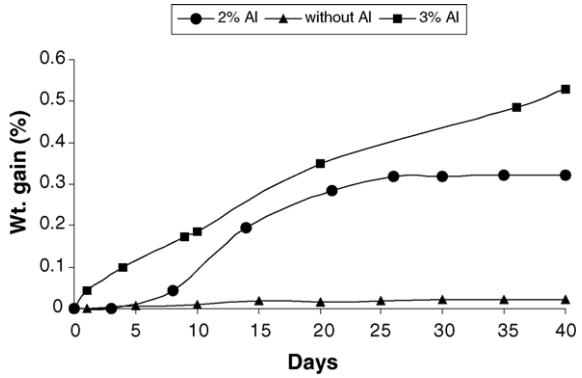

Fig. 2. Weight changes of MgO–C samples, coked at 1050 °C for 3 h, in air with time.

cracks without crumbling, accompanied by a smaller percent gain in weight, and samples without Al neither developed any cracks nor gained in weight after 30 days of exposure. Therefore, it may be concluded that Al content has a decisive role in the disintegration of MgO–C bricks on exposure to moist air.

To identify the phases responsible for disintegration, XRD analysis was conducted on MgO–C sample containing 3% Al immediately after coking (Fig. 4). Periclase and graphite are the main phases while aluminium carbide (Al_4C_3) aluminium oxycarbide (Al_4O_4C) and aluminium are minor phases and the percent of Al_4C_3 was found as low as 0.4%. Disintegrated powder samples after 30 days exposure was also analysed by XRD but no additional phases were identified.

To understand the mechanism of disintegration, it was decided to prepare Al_4C_3 or similar phases and study their disintegration behaviour. Further studies were conducted with samples containing only Al and C in the molar proportion of 4:3.

3.2. Disintegration of coked Al–C samples

Al–C samples were coked 3 h at 1050 °C and exposed in air at ambient temperature. Fig. 5 shows the plot of %weight gain of Al–C sample versus days of exposure in open atmosphere. It was observed that the percent weight gain reached a maximum of 16% in 60 days and remained constant thereafter. Fig. 6(a)–(c) show the progressive superficial changes of Al–C coked samples on exposure to air for 1 day, 15 days and 22 days respectively. As compared to the MgO–C samples containing 3 wt.% Al (Fig. 3), these samples crumbled faster (in 10–15 days) and virtually became dust in 22 days. Moreover, the %weight gains of Al–C samples are much greater (16 wt.%) as compared to about 0.5 wt.% in MgO–C samples with 3 wt.% Al (Fig. 2) in 40 days exposure. This is attributed to the fact that the %Al is lower and consequently the phases produced in MgO–C–Al samples are much lower in amounts compared to those of Al–C samples coked at same temperature and exposure of

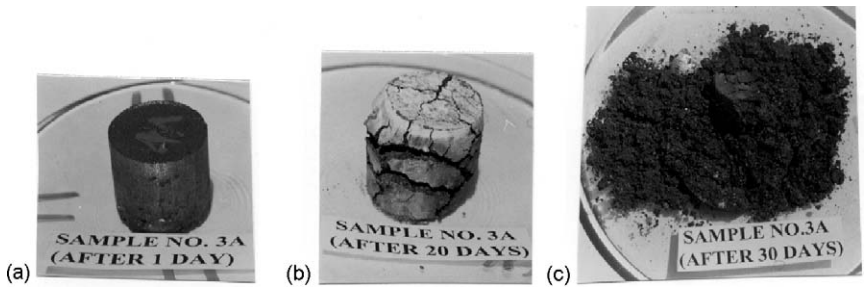

Fig. 3. Photographs of MgO–C samples having 3% Al after exposure for (a) 1 day; (b) 20 days; and (c) 30 days.

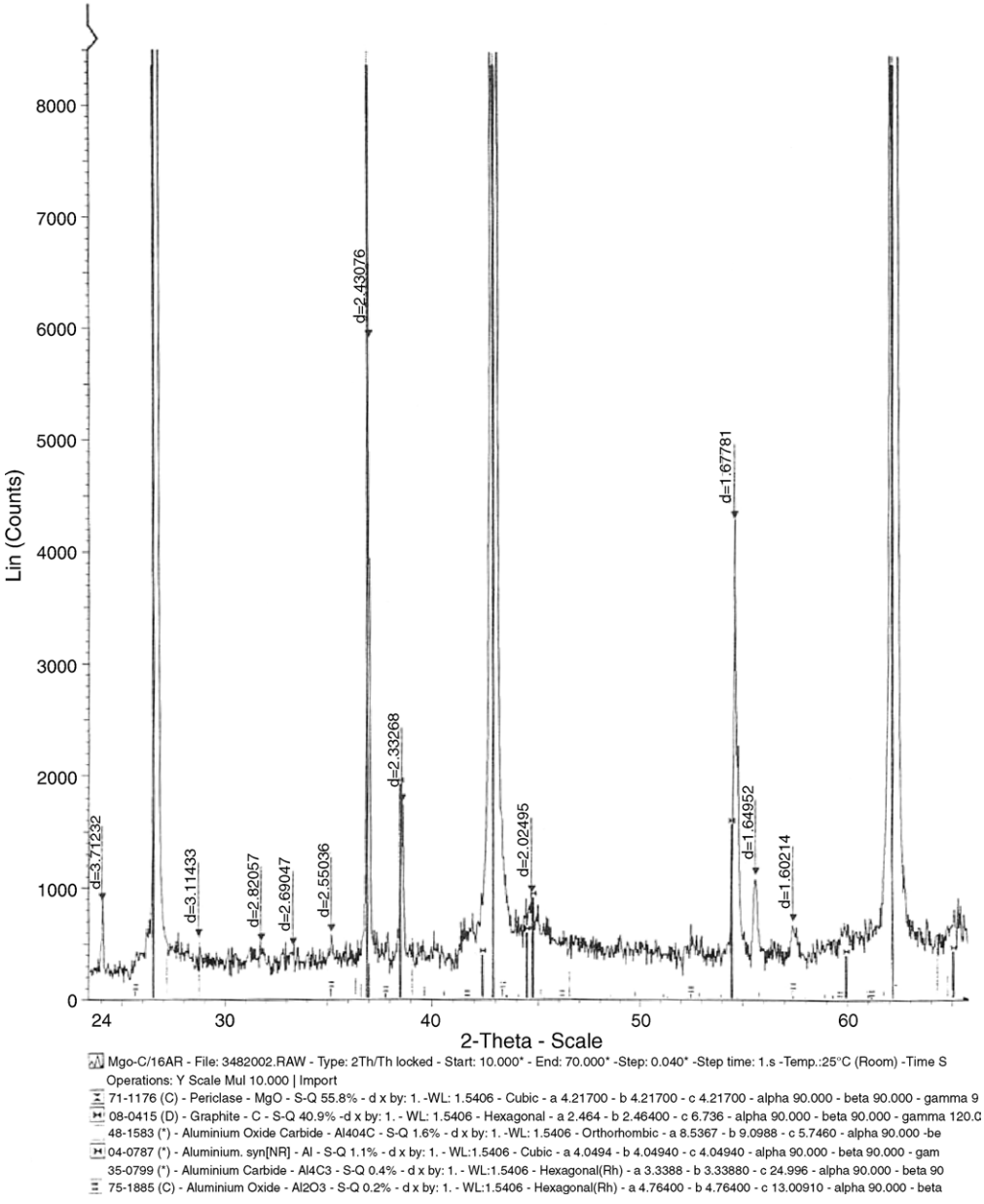

Fig. 4. XRD of MgO–C (3% Al) sample after coking at 1050 °C for 3 h.

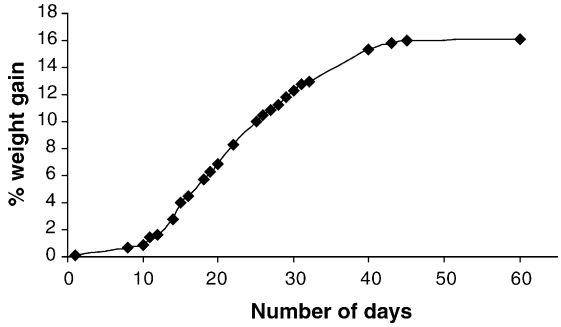

Fig. 5. %Weight gain of a typical coked Al–C sample as a function of time of exposure in open atmosphere.

Table 2
Percentage analysis of different phases present in XRD tests

Phase	Before exposure	After exposure	
		As analyzed	After graphite correction
Graphite	74.3	86.7	74.3
Al	5.1	2.7	2.2
Al_2O_3-monoclinic	3.6	1.5	1.2
Al_4C_3	13.9	7.2	6.1
Al_4O_4C	3.1	1.8	1.5
Additional amorphous phase	–	–	14.7
Total	100	99.9	100

same period of time. Therefore, higher %weight gain and earlier crumbling of the coked Al–C samples on exposure to moist atmosphere are attributed to the higher content of product phase(s) which arises during coking.

For identification of these phases, XRD analyses were conducted with powdered Al–C samples after coking and also with disintegrated powder after exposure in air for 60 days.

3.3. X-ray diffraction study

It is observed from Fig. 7(a) and (b) XRD analysis that major phase present in both the cases is graphite. Other minor phases are Al_2O_3, Al_4C_3 and Al_4O_4C and aluminium. Semi-quantitative analysis shows the relative percentages of these phases. Table 2 indicates percentages of these phases. It is interesting to note that amount of graphite is more in exposed sample. It is expected that graphite had not taken part in certain reactions responsible for disintegration of Al–C samples and therefore its percentage should remain constant. This is only possible if we consider that some amorphous phases had formed due to reaction in prolong exposure in air. Percentages of different phases after correction for graphite are also indicated in the Table 2. It is interesting to note that percentage of unidentified amorphous phase (14.7%) in disintegrated sample is very close to weight increase (16%) as observed due to exposure of coked sample in air for 60 days.

From the above results, it is seen that percentage of Al, Al_2O_3, Al_4C_3 and Al_4O_4C has reduced after exposure of the coked sample to atmosphere for 60 days and it seems that these phase have been converted to some other amorphous phase(s). It is interesting to note that in addition to carbides (earlier reported) percent reduction of alumina and aluminium has taken place. It is reported [10] that a protective layer coating of Al_2O_3 is formed on Al (aluminium) and this protective coating is broken during heating to >650 °C. Al thus exposed can react with carbon or atmospheric oxygen or nitrogen. After cooling the part of residual unreacted Al reacts with moisture to form hydroxides of Al [11]. In order to know the nature of these amorphous phases, IR studies were conducted with coked Al–C samples before and after exposure to atmosphere.

3.4. Infrared study of the Al–C samples

Fig. 8(a) and (b) shows infrared spectrum of Al–C sample after coking as well as after exposure in open atmosphere for 60 days. In infrared, frequency of 3700–2500 cm^{-1} is defined as X–H stretching where X = C, N, O, S. In both the IR plots of Fig. 8, this stretching frequency peak are visible at 3462 cm^{-1} which is characterised as OH^- stretching and also at 1635 cm^{-1} for bending of H_2O. However, these peaks are more distinct in sample after 60 days of exposure to atmosphere (Fig. 8(b)). IR spectrum of sample after coking (Fig. 8(a)) only shows the presence of minor OH stretching at 3462 cm^{-1}. The above evidence suggests that the product phase(s), obtained after the completion of coking, possibly undergoes hydration and this hydration process starts immediately after exposure to atmosphere. The large peak at 3462 cm^{-1} after 60 days of exposure to atmosphere suggests continuation of this hydration process to generate more hydrated product.

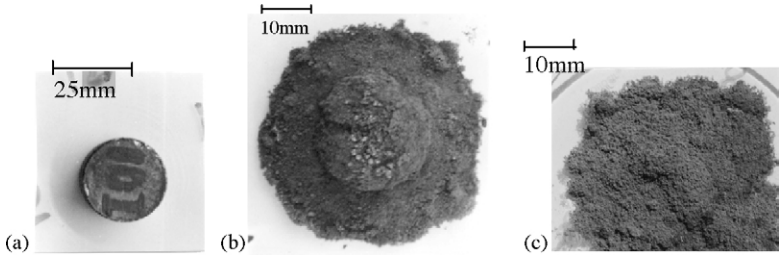

Fig. 6. Photographs of Al–C samples coked at 1050 °C for 3 h, after exposure in air for (a) 1 day; (b) 15 days; and (c) 22 days.

3.5. Effect of oxygen on the coked Al–C samples

To further confirm the finding that hydration is responsible for disintegration and weight increase, the coked Al–C sample was exposed to moisture-free oxygen for 60 days and weight changes was recorded at regular interval. Fig. 9 shows slight gain of weight (0.1%) of sample kept in moisture-free O_2 for 60 days as compared to 16% weight gain observed for the similar sample on exposure to air for the same period of time. Further, no crack formation or any disintegration of sample was observed during these 60 days of experiment. Therefore, it can be concluded that oxygen has no role on the disintegration process of coked Al–C samples. On the contrary, presence of moisture is essential for weight gain and disintegration (Figs. 3 and 6). This further establishes the earlier finding that the hydration of product phases is responsible for the disintegration.

3.6. Scanning electron microscope (SEM) and EDS study on Al–C sample

Further investigations were carried out with coked Al–C sample under SEM and EDS. Fig. 10 shows the SEM photographs of the powdered Al–C sample after coking. Fig. 10(a) shows that feather like structures are stacked together. However, in different location it is seen that similar structure have gradually reacted from the top and disintegrated as shown clearly in Fig. 10(b). It appears particularly from the Fig. 10(b) that the morphology of stack is hexagonal and the size is about 10 μm. On the contrary, the product

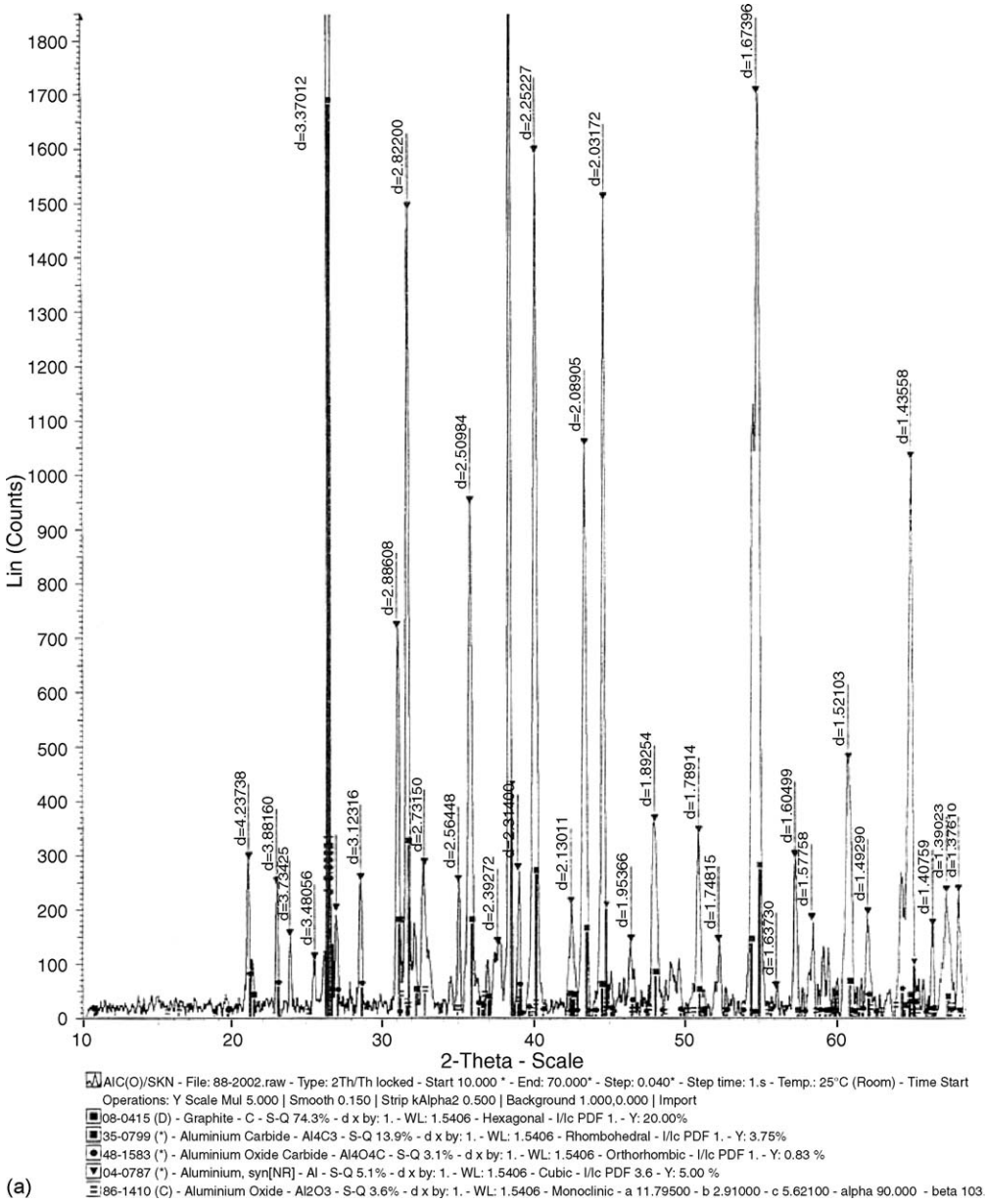

(a)

Fig. 7. XRD of Al–C sample (a) after coking at 1050 °C for 3 h and (b) coked at 1050 °C for 3 h, after 60 days in open atmosphere.

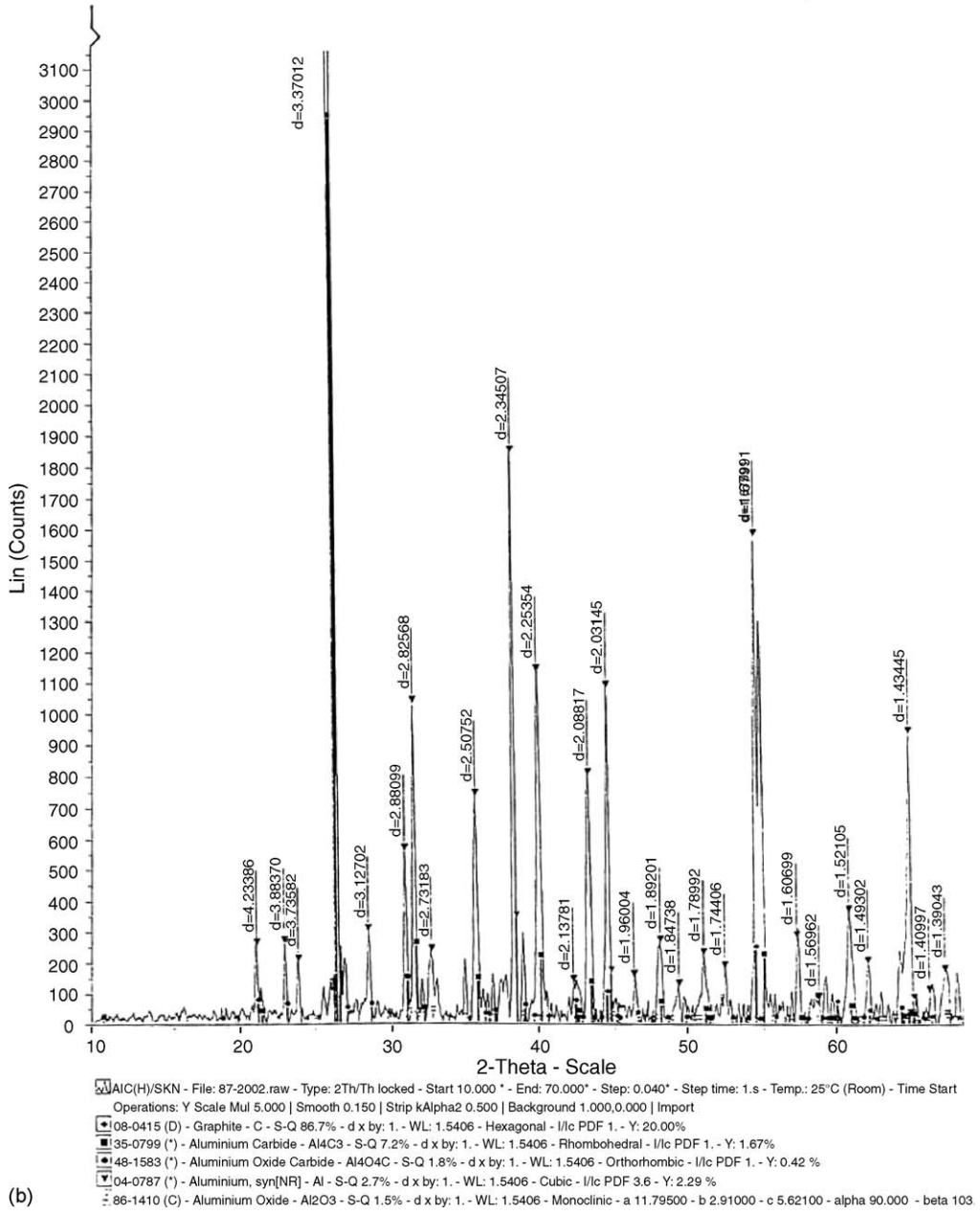

Fig. 7. (*Continued*).

phase due to hydration on exposure to atmosphere is so very fine in size that the particles could not be resolved by SEM photograph. In EDS spectra of the above stack-like structures, it is seen that Al is present in both the cases.

3.7. Electron probe micro analysis

Further investigation was carried out with the same sample under EPMA. Fig. 11 shows EPMA photographs of the stack-like structure. It is seen from Al, O and C scan that Al and O are present in the stack-like structure but no carbon is present. Based on earlier XRD results, it can be said that the stack-like structure is Al_2O_3 and it is disintegrating due to hydration (Fig. 10(b)). The above phenomena of disintegration of Al_2O_3 were not referred by earlier authors [8,9]. It is interesting to note from XRD results that the percentage of Al_2O_3, Al_4C_3, Al_4O_4C and Al has decreased after exposure to moisture. While IR studies has confirmed presence of OH^- containing phases. Therefore, hydration mechanism was analysed from thermodynamic point of view.

3.8. Thermodynamics of the quaternary Al–O–H–C and ternary Al–O–H system

In order to thermodynamically explain the disintegration of MgO–C–Al bricks on exposure to atmospheric moisture, two stability diagrams of the systems Al–O–H–C and Al–O–

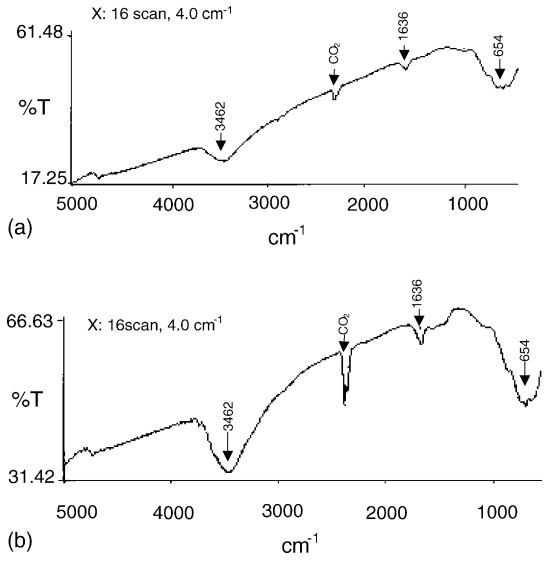

Fig. 8. IR spectrum of (a) Al–C samples coked at 1050 °C for 3 h and (b) coked Al–C samples after 60 days of exposure in air at ambient temperature.

H have been drawn for room temperature (298 K). The following standard free energy changes (ΔG°) [12] have been used to draw the diagrams.

$$2Al(s) + 1.5O_2(g) = Al_2O_3(s); \Delta G^\circ = -1,675,700 + 313.35T \text{ J} \quad (1)$$

$$4Al(s) + 3C(s) = Al_4C_3(s); \Delta G^\circ = -209,200 + 41.4T \text{ J} \quad (2)$$

$$Al(s) + 1.5O_2(g) + 1.5H_2 = Al(OH)_3(s); \Delta G^\circ = -1,293,250 + 461.7T \text{ J} \quad (3)$$

$$H_2(g) + 0.5O_2(g) = H_2O(g); \Delta G^\circ = -241,800 + 44.45T \text{ J} \quad (4)$$

$$C(s) + 2H_2(g) = CH_4(g); \Delta G^\circ = -74,800 + 80.6T \text{ J} \quad (5)$$

Since, according to Eq. (2), in a carbon-saturated system at 298 K, solid aluminum carbide (Al_4C_3) is a stable phase

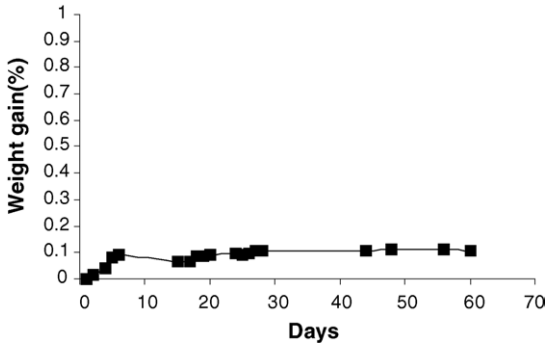

Fig. 9. Plot of %weight gain vs. time in days of at 1050 °C exposed to moisture-free flowing oxygen.

and solid aluminium (Al) is a metastable one, it is thermodynamically impossible to show the stability field of Al in the C-saturated quaternary (Al–O–H–C) diagram. However, since the XRD analysis of the coked Al–C samples showed the presence of Al with those of Al_4C_3, Al_2O_3 and C (Fig. 7(a)), two separate stability diagrams have been drawn; one, which is a quaternary (Al–O–H–C) and shown in Fig. 12(a), involving Al_4C_3 (solid) in a carbon-saturated system, and the other, which is a ternary (Al–O–H) and shown in Fig. 12(b), involving Al (solid) and no carbon. Fig. 12(a) shows the stability fields of Al_2O_3 (solid), Al_4C_3 (solid) and Al $(OH)_3$ (solid), each accompanying carbon (solid), with log p_{CH_4} and log p_{H_2O} being the two variables plotted. Point T, with log $p_{CH_4} = 97.14$ and log $p_{H_2O} = -2.53$, represents the triple point, at which the three solid phases Al_2O_3, Al_4C_3 and $Al(OH)_3$ coexist with the solid carbon and the gas phase. The atmospheric condition ($p_{H_2O} = 0.014$ atm and $p_{CH_4} \approx 0$) is given by the point S, at which the thermodynamically stable phase is $Al(OH)_3$, the formation of which causes the crumbling of the bricks. The conversion of Al_2O_3, due to atmospheric exposure, into $Al(OH)_3$, according to the following equations, is a direct, one stop process, as can be seen from Fig. 12(a).

$$Al_2O_3(s) + 3H_2O(g) = 2Al(OH)_3(s) \quad (6)$$

In contrast, Al_4C_3 does not directly convert into $Al(OH)_3$ following the reaction given below.

$$Al_4C_3(s) + 12H_2O(g) = 4Al(OH)_3(s) + 3CH_4(g) \quad (7)$$

As shown in Fig. 12(a), when Al_4C_3 is exposed to the atmospheric condition (S), the equilibrium state of Eq. (7) does not lie on the stable segment, TD, of the equilibrium; instead, it falls at E on the metastable segment, TM, of the equilibrium, where Al_2O_3 is the stable phase. The state E ($p_{CH_4} = 0.0035$ atm, $p_{H_2O} \approx 0$) has been thermodynamically calculated using the starting atmospheric composition, given by point S, and the equilibrium constant of reaction (7). The gas composition moves from the initial state (S) to the final state (E) along the line SE under the combined effect of a decrease in p_{H_2O} and an increase in p_{CH_4}, both shown by the arrowheads in Fig. 12(a). Thus, it may be concluded that both Al_2O_3 and Al_4C_3, when exposed to atmospheric moisture, convert into $Al(OH)_3$; Al_2O_3 converts directly, while Al_4C_3 converts through the intermediate formation of Al_2O_3.

The stability field of aluminium oxycarbide (Al_4O_4C), which must interpose between those of Al_2O_3 and Al_4C_3, has not been included in Fig. 12(a) to avoid the complexity of stage wise calculations to determine the final state, E. The aforesaid conclusions remains unchanged even when the oxycarbide is incorporated into the figure.

Fig. 12(b), which can be explained in the same manner as Fig. 12(a), presents the stability fields of Al (solid), Al_2O_3 (solid), and $Al(OH)_3$ (solid), with $-\log p_{O_2}$ and log p_{H_2O} being the two variables plotted. In this case, it can be

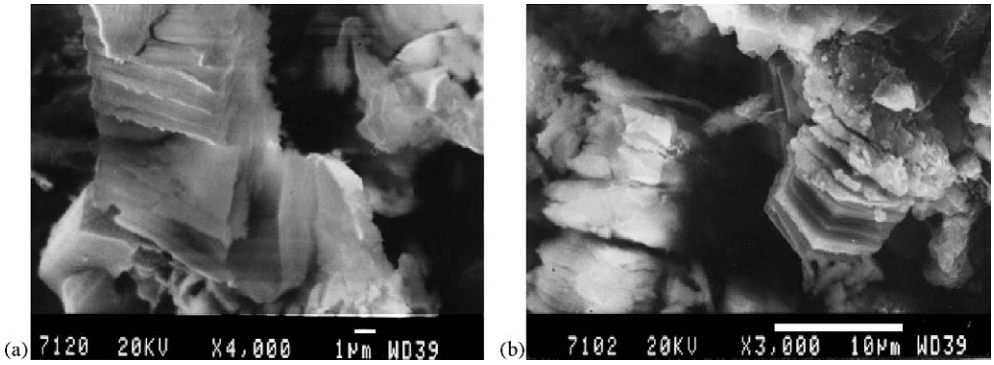

Fig. 10. SEM photograph of sample (a) before and (b) after exposure to atmosphere.

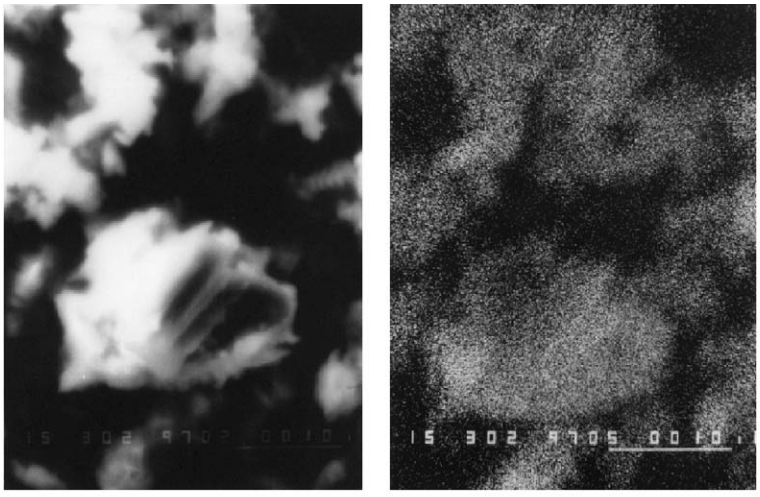

(a) SEI X 3000 (b) Al X - ray dot map

(c) : C, X-ray dot map (c) : C, X-ray dot map

Fig. 11. EPMA of Al–C samples after coking at 1050 °C and exposure in atmosphere for 60 days.

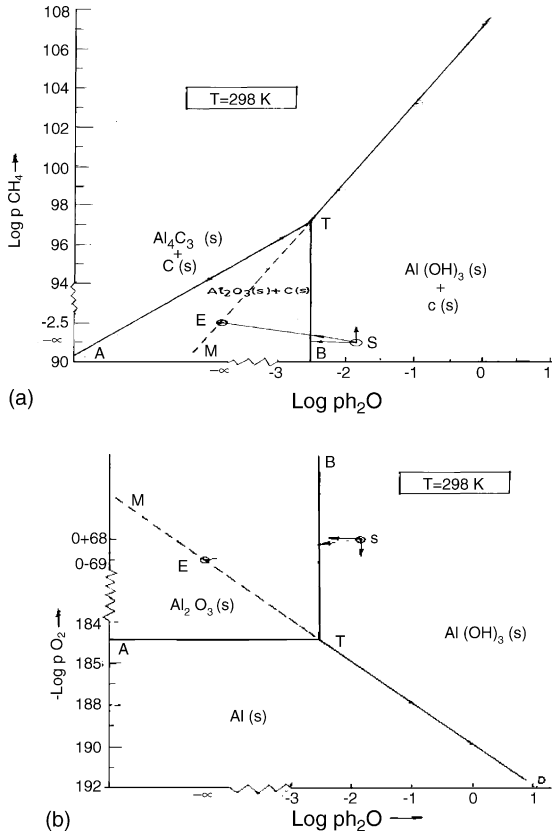

Fig. 12. Stability diagram of (a) the C-saturated quaternary system Al–O–H–C and (b) the ternary system Al–O–H at 298 K

concluded from the figure that both Al and Al_2O_3, when exposed to atmospheric condition ($p_{O_2} = 0.21$ atm and $p_{H_2O} = 0.014$ atm), represented by point S, convert into Al $(OH)_3$; Al_2O_3 converts directly as in Fig. 12(b), while Al converts through the intermediate formation of Al_2O_3, as indicated by point E ($p_{O_2} = 0.207$ atm and $p_{H_2O} \approx 0$), lying on the metastable segment (TM) of equilibrium (3).

From the above discussion based on the experimental results of the Al–C coked samples before and after exposure to atmosphere, it can be concluded that the phase of the coked sample, e.g. Al_4C_3, Al and Al_2O_3 on exposure to moist air undergo hydration giving rise to $Al(OH)_3$ and ultimately causes the cracking and dusting of the sample.

4. Conclusions

MgO–C–Al bricks fired in reducing condition disintegrates on prolong exposure to moisture while Al–C samples coked at 1050 °C showed much higher degree of disintegration occurred when exposed to atmosphere at the ambient temperature.

(i) XRD analysis revealed formation of Al_4C_3, Al_4O_4C and Al_2O_3 in coked sample and reduction of their amount along with formation of additional amount of amorphous phase after exposure to ambient atmosphere.

(ii) IR studies on disintegrated material confirmed presence of OH^- ion, which indicates that hydration, is responsible for disintegration.

(iii) Exposure of coked Al–C sample under moisture-free oxygen showed no cracks or crumbling, which further confirmed that disintegration is due to hydration.

(iv) SEM analysis showed disintegration of stack-like structure due to hydration. EDS analysis indicated that the stack-like structure is a phase having Al in it. EPMA analysis confirmed that the above phase is a compound of aluminium and oxygen. Carbon is not present in this phase. Based on earlier XRD results, it can be said that the stack-like structure is Al_2O_3 and it is disintegrating due to hydration.

Acknowledgements

The authors are grateful to the management of RDCIS, SAIL, for their kind permission for publication of the article. The authors also convey sincere thanks to the management of Jadavpur University. Help received from Shri C.B. Sharma, RDCIS for SEM studies, Shri B.B. Patra for EPMA and Shri K. Kumar for XRD studies are gratefully acknowledged.

References

[1] R. Brenzy, C.E. Semler, Oxidation and diffusion in selected pitch-bonded magnesia refractories, J. Am. Ceram. Soc. 67 (1984) 480–483.
[2] K. Tabata, H. Nishio, K. Itoh, A study on oxidation–reduction in MgO–C refractories, Taikabutsu Overseas 8 (1988) 3–10.
[3] N.K. Ghosh, D.N. Ghosh, K.P. Jaganathan, Oxidation mechanism of MgO–C in air at various temperatures, Br. Ceram. Trans. 99 (3) (2000) 124–128.
[4] A. Watanabe, H. Takashi, S. Takanaga, N. Goto, K. Anan, M. Uchida, Behavior of different metals added to MgO–C bricks, Taikabutsu Overseas 7 (1987) 17–23.
[5] K. Ichikawa, H. Nishio, O. Nomura, Y. Hoshiyama, Suppression effects of aluminum on oxidation of MgO–C bricks, Taikabutsu Overseas 15 (1995) 21–24.
[6] S. Hanagiri, T. Harada, S. Aso, S. Fujihara, H. Yasui, S. Takanaga, H. Takahashi, A. Watanabe, Effects of addition of metal and CaB_6 to magnesia carbon bricks for converters, Taikabutsu Overseas 13 (1993) 20–27.
[7] H. Toritani, T. Kawakami, H. Takahashi, I. Tsuchiya, H. Ishh, Effect of metallic additives on the oxidation–reduction reaction of magnesia–carbon brick, Taikabutsu Overseas 5 (1985) 21–27.
[8] O. Benhui, W. Ruikun, W. Zhougxian, The effects of non-metal additives on hydration resistance of MgO–C bricks, Chin. Refractories 9 (2000) 29–31.
[9] P.T. Trowell, Evolution of magnesia–carbon refractories, Ceram. Ind. Feb. (1995) 41–45.
[10] C. Taffin, J. Poirier, The behaviour of metal addition in MgO–C and Al_2O_3–C refractories, Interceram 43 (1994) 354–358.
[11] T.R. Ramachandran, Raw materials for alumina ceramics, Indian Ceram. Soc. 54 (4) (1995) 117–123.
[12] O. Kubaschewski, C.B. Alcock, P.J. Spencer, Materials Thermo-Chemistry, sixth ed., Pergamon Press, Tarrytown, NY, 1993pp. 258–323.